



Surface enhanced Raman scattering spectroscopy of Ag nanoparticle aggregates directly photo-reduced on pathogenic bacterium (*Helicobacter pylori*)

Hayato Kudo^a, Tamitake Itoh^{b,*}, Takehiro Kashiwagi^a, Mitsuru Ishikawa^b, Hiroaki Takeuchi^c, Hiroyuki Ukeda^{a,*}

^a Faculty of Agriculture, Kochi University, Monobe B-200, Nankoku 783-8502, Japan

^b Nano-bioanalysis Group, Health Research Institute, National Institute of Advanced Industrial Science and Technology (AIST), Takamatsu, Kagawa 761-0395, Japan

^c Department of Clinical Laboratory Medicine, Kochi University School of Medicine, Nankoku, Kochi 783-8505, Japan

ARTICLE INFO

Article history:

Available online 31 March 2011

Keywords:

SERS
Ag nanoparticle aggregates
Photo-reduction
Bacterial surfaces (*Helicobacter pylori*)

ABSTRACT

To enable us surface enhanced Raman scattering (SERS) spectroscopic detection of bacteria having low affinity for Ag colloidal nanoparticles, we examined simple experimental methodology; SERS detections using Ag nanoparticles aggregates directly synthesized by photo-reduction on the surfaces of such bacteria (*Helicobacter pylori*). The synthesized Ag nanoparticles aggregated on bacterial surfaces and generated temporally and spectrally fluctuated SERS spectra that are tentatively attributed to amide groups of surface proteins. The selective appearance of amide groups and fluctuation in SERS spectra indicated chemical contribution to SERS. By referring to previous reports, we estimated total SERS enhancement factors to be $\sim 10^{11}$. Electromagnetic (EM) enhancement factors of SERS are up to $\sim 10^8$. Thus, we considered that chemical ones may be $< \sim 10^3$ in the present SERS active system.

© 2011 Elsevier B.V. All rights reserved.

1. Introduction

Molecular discrimination of bacterial cell surfaces is important to know biological cell information including cell cycling and so on [1,2]. Several spectroscopic methods enable us to identify cell surface molecules. In particular, Raman scattering spectroscopy is a potential method, because detailed vibrational spectra of Raman scattering are useful for well-defined discrimination of molecular species [1,2]. However, cross-sections of Raman scattering (ca. 10^{-30} cm²) is too low compared with absorption cross-sections of fluorescence (ca. 10^{-16} cm²). Thus, Raman scattering has disadvantage in the detection sensitivity. SERS on the other hand resolves this disadvantage by signal enhancement by the factors of 10^{10} – 10^{14} for the molecules located at junctions of SERS-active Ag and Au nanoparticle aggregates [3–6]. To-date two mechanisms are proposed for accounting enhancement factor in SERS: EM mechanism and chemical mechanism [7,8]. EM mechanism is characterized by twofold EM enhancement of Raman signals by plasma (plasmon) resonance of Ag and Au nanoparticle aggregates [9–12]. Chemical enhancement is characterized by shifting Raman scattering in non-resonance to

that in resonance by forming charge transfer complexes between molecules and surfaces of Ag and Au nanoparticle aggregates [13–17]. Ultrahigh sensitivity of SERS enables us to measure Raman spectra of a single biomolecule [18,19]. Thus, SERS is now extensively used for probing and analyzing intracellular and extracellular components [20–27]. Nevertheless, affinity of molecules for Ag and Au surfaces is a primary requirement for accomplishing large enhancement. This requirement limits ability of SERS to various fields. Indeed, single molecule SERS detections have been carried out using molecules whose functional groups (i.e., amino and thiol group) have high affinity for Ag and Au surfaces [28,29].

Helicobacter pylori (*H. pylori*), one of the most widely known pathogenic bacteria, is Gram-negative spiral-shaped bacterium and is causative agent to varieties of *H. pylori*-associated diseases such as chronic idiopathic thrombocytopenic purpura and gastroduodenal disorders including gastric cancer and gastric B-cell lymphoma [30]. Interaction between *H. pylori* and the host (gastric epithelium) is critical event on the development of persistent infection, host immunoresponse (inflammations) and pathogenesis. *H. pylori* has unique characteristics; morphologically converting short-rod to coccoid form and cell aggregation are observed due to adaptation to microenvironment (*in vivo* and *in vitro*). The bacterial molecules localized and distributed on cell surface of *H. pylori* are considered to be involved in such biological behaviors (bacterium–host interaction and microbiological characteristics) in the human stomach.

* Corresponding authors. Tel.: +81 87 869 3557; fax: +81 87 869 4113.

E-mail addresses: tamitake-itou@aist.go.jp (T. Itoh), hukeda@kochi-u.ac.jp (H. Ukeda).

In this study, in order to resolve the limitation of SERS by directly preparing Ag nanoparticles on the surface of *H. pylori* by photo-reduction and detected SERS spectra from Ag nanoparticles aggregates (Ag NPs). On the other hand, *H. pylori* does not show affinity for externally added Ag nanoparticles. The key of the current work is that Ag nanoparticles can be directly prepared on the surface of *H. pylori* by focusing green laser in a suspension of bacteria in a solution of mixture of silver nitrate and citric acid. Under continuous irradiation of the above suspension, aggregates of bacteria began to show SERS signals from Ag nanoparticles produced on their surfaces.

2. Experimental

Silver nitrate and trisodium citrate dehydrate were purchased from Wako Pure Chemical Industries (Osaka, Japan). *H. pylori* strain HPK5, obtained from a patient with gastric ulcer [31] has been used for the current work. Living *H. pylori* cells suspended in sterilized water were placed under aerobic condition for more than overnight at room temperature. After death of microorganisms was confirmed by count of colony forming unit (CFU), the cell suspensions were moved to SERS measurement room for which the regulation is at bio-safety level 1. Then, Ag nanoparticles were adsorbed on bacteria by two methods. The first method is illustrated in Fig. 1 A and B. Briefly, colloidal solutions of Ag nanoparticles (~40 nm in diameter, 9.6×10^{-11} M) were prepared by Lee–Misel method [34]. After the preparation of colloidal solution, the concentration of Ag nanoparticles was increased by 10 times using centrifugation (13,000 rpm, 5 min). After removal of supernatant, the remaining 100 μ L of concentrated colloidal solution was added to 900 μ L of the cell suspension. An aliquot of the mixture was dropped on a slide glass, covered by cover slip to protect evaporation and incubated for 1 h for spontaneous adsorption of Ag nanoparticles to bacterial surfaces. The second method is illustrated in Fig. 1 C and D. Briefly, 500 μ L of the cell suspension was added to 500 μ L of 2 mM Ag nitrate and citric acid mixture solution. An aliquot of the mixture was dropped on a slide glass, covered by cover slip and then irradiated with cw diode green laser light (260 W/cm²) to synthesize directly Ag NPA on bacterium surfaces by photo-reduction. Details of this method are provided in the next paragraphs. Samples were placed on the stage of an inverted optical microscope (Olympus IX70), and a collimated unpolarized white light beam from a 100 W halogen lamp was introduced into the sample through a dark field condenser lens. A cw diode laser (Coherent DPSS 532, Palo Alto, CA; 532 nm 16 mW) was used for SERS excitation in the first method. A cw diode pumped green laser was used for both photo-reduction and SERS excitation in the second method. The focusing area of the cw diode laser light was 6100 μ m². A holographic notch filter was placed behind an objective lens (Olympus LCPlanF1, 60 \times , NA 0.7) to block Rayleigh light. SERS was detected using either a digital camera (Nikon, COOLPIX5000) for imaging or using a charge-coupled device (Andor, DV434-FI) equipped with a polychromator (Acton, Pro-275) for spectral measurements [35]. Exposure time for one measurement was 2 s. Movies of blinking SERS images were taken by a CCD camera (Mintron, MTV-63V6HN) with 0.25 s temporal resolution. High spatial resolution imaging of *H. pylori* immobilized on a slide glass and adsorbed with Ag nanoparticles was acquired by field emission scanning electron microscope (FE-SEM, JEOL, JSM-6700FZ, ultimate resolution 1.0 nm) operating at 10 μ A and 15 kV. SEM images were acquired after drying the samples for 24 h under vacuum and coating with osmium using an osmium coater (Vacuum Device Inc., HPC-1SW). To identify aggregates of Ag nanoparticles adsorbed onto the surfaces of bacteria, dispersive X-ray spectrometry (EDS, JEOL, JED-2300) operating at 20 μ A and 20 kV was used.

3. Results and discussion

Fig. 1a shows a dark field image of *H. pylori* in the Ag colloidal solution. By focusing green laser (260 W/cm²) on several single cells we could not observe any SERS light spot from the surfaces of single cells. We consider the failure of SERS observation due to low amount of Ag nanoparticles adsorbed on bacteria, because molecules located at junctions of Ag nanoparticles dimers can generate detectable SERS signals. Indeed, Fig. 1a shows that only one or two Ag nanoparticles are adsorbed on each *H. pylori* cell. Thus, to increase the total amount of Ag nanoparticles adsorbed on bacteria in the view field of the microscope (in other words, to increase the possibility of finding out Ag nanoparticle dimers on bacteria), the aggregates of *H. pylori* composed of c.a. 10,000 cells were subjected to this way. Fig. 1b shows a dark field image of a *H. pylori* aggregate (HPA) in the Ag colloidal solution. By focusing green laser (260 W/cm²) on the HPA, several SERS light spots were observed as indicated by circles in Fig. 1c, however we failed to measure their SERS spectra because of instability of SERS light spots. SERS light spots were always quenched before starting spectral detections. In order to overcome the problems of low amount of adsorbed Ag nanoparticles and instability of SERS light spots, we directly synthesized Ag NPs on bacterial surfaces by a photo-reduction method [36–38]. Fig. 1d shows the dark field image of several bacteria in the mixture of Ag nitrate and citric acid. In this case of single bacterium, even the adsorption of Ag nanoparticles we could not measure SERS spectrum by the common problem. Thus, we selected a HPA as shown in Fig. 1e and focused laser on it to increase the number of SERS light spots. Interestingly as shown in Fig. 1f, we observed a large number of SERS light spots on the HPA. The appearance of many SERS light spots indicates that HPAs acting as strong light scatter enhanced the efficiency of photo-reduction of Ag nitrate. We consider that Ag NPs were synthesized at bacterial surface molecules whose functional groups have high affinity with Ag atoms. We should remove the possibility that SERS light spots in Fig. 1f are from citric acid because SERS activity of citric acid is reported [39,40]. As shown in the insets of Fig. 1e and f, we prepared a large Ag NPA whose size is similar to that of HPAs by adding the dense sodium chloride solution (5 M; final concentration). The Ag NPA just showed only negligible SERS light spots compared with that of HPAs because our laser power (260 W cm²) may be much lower than the reported ones [39,40]. Thus, SERS spectral intensity from citric acid in the present measurements may be negligibly small and the SERS light spots in Fig. 1f are from Ag NPs adsorbed on the bacterial ingredients.

FE-SEM was carried out to confirm the adsorption of Ag NPs on HPA. Fig. 1g and h shows SEM images corresponding to the images of Fig. 1c and f, respectively. Few Ag NPs were observed in only small area indicated by a circle (Fig. 1g), however many Ag NPs were observed on the surface of the HPAs when utilized with this direct photo-reduced method (Fig. 1h). To determine whether these Ag NPs detected are “real” Ag NPs, EDS was analyzed, demonstrating that EDS spectra from inside (Fig. 1i) and outside (Fig. 1j) an orange circle in Fig. 1h. (For interpretation of the references to color in this figure, the reader is referred to the web version of the article.) The EDS spectrum with significant peak at 3.0 keV was observed from inside (Fig. 1i) but not outside (Fig. 1j) indicating that Ag atoms in the circle were really existed and definitely detected. The same results were obtained from analyses with the objects of Fig. 1g. Taken together, this method developed could capture the true Ag NPs adsorbed on the HPA.

We measured SERS spectra from a several bright light spots on HPAs as indicated in Fig. 1f. Fig. 2A shows the six SERS spectra measured from the different spots. In spectra “a”–“f”, several significant bands located around 1200–1700 cm⁻¹. Interestingly, all spectra have mainly two outstanding SERS bands, for example

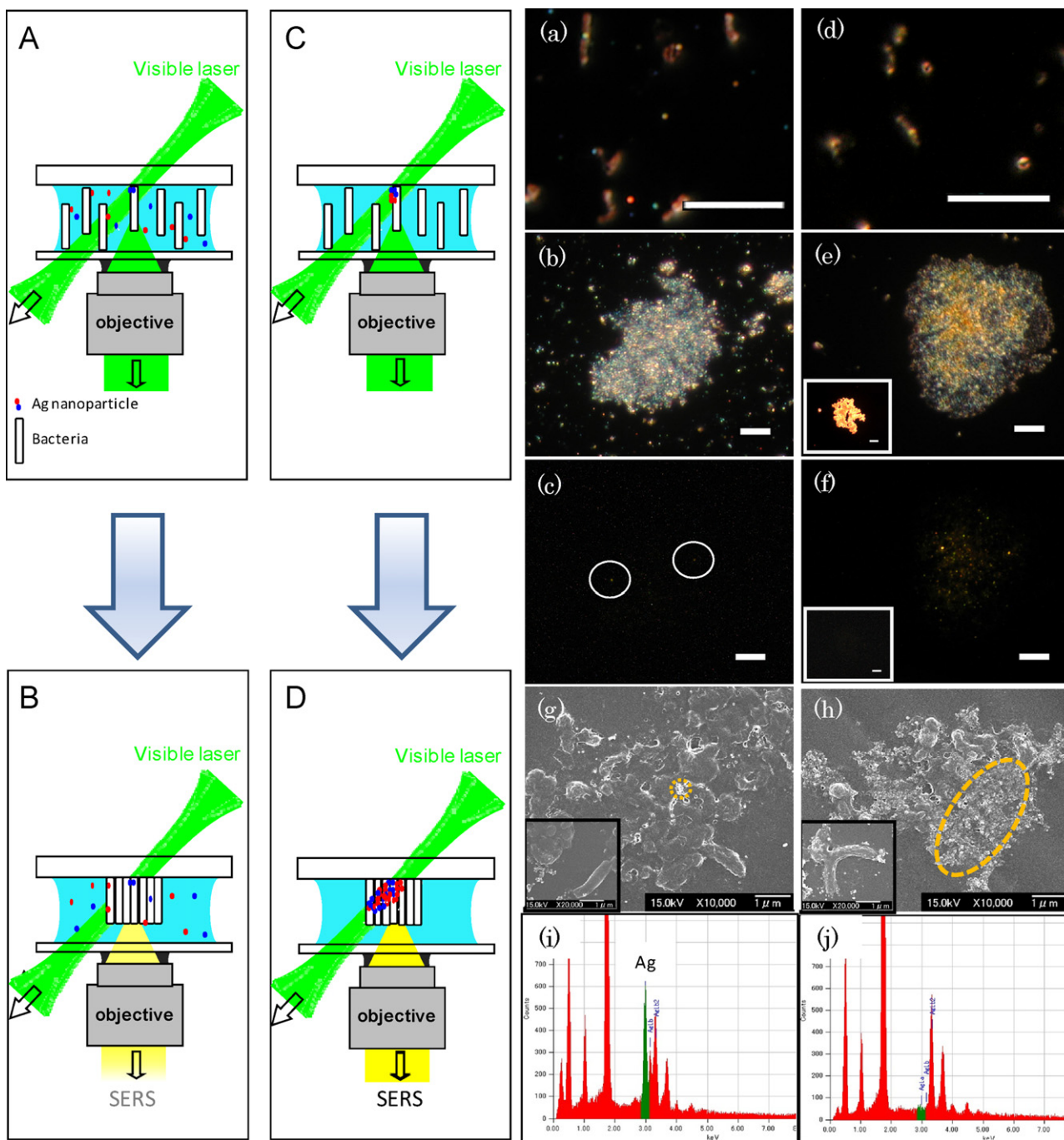


Fig. 1. (A) Schematics of an experimental procedure for SERS measurements of a single bacterium using Ag colloidal nanoparticles, (B) that for SERS measurements of a bacterial aggregate using Ag colloidal nanoparticles, (C) that for SERS measurements of a single bacterium using photo-reduction of silver nitrate, and (D) that for SERS measurements of a bacterial aggregate using photo-reduction of silver nitrate. (a) A dark field image of isolated single bacteria in Ag colloidal solution, (b) that of a bacterial aggregate in Ag colloidal solution, (c) a SERS image of a bacterial aggregate in Ag colloidal solution, (d) a dark field image of isolated single bacteria in Ag nitrate solution, (e) that of a bacterial aggregate in Ag nitrate solution, (f) a SERS image of a bacterial aggregate in Ag nitrate solution. Inset of (e) and (f): a dark field image and a SERS image of a large Ag nanoaggregate with citric acid. Scales of (a)–(f) are all 10 μm . (g) A SEM image of a bacterial aggregate with Ag colloidal nanoparticles and (h) that of a bacterial aggregate with Ag nitrate after laser irradiation. Inset of (g) and (h) enlarged image of single bacteria. (i and j) EDS spectra inside and outside an orange circle with dashed line on bacterial aggregates in (g and h), respectively.

Fig. 2Aa shows the bands at 1388 and 1654 cm^{-1} and Fig. 2Ab at 1303 and 1621 cm^{-1} . The spectral fluctuation of both SERS bands is discussed elsewhere. The SERS bands in the spectral regions are tentatively attributed to amide groups (CO–NHs) as previously reported [19,41–45]. Indeed, the surface of *H. pylori* cells has many important components such as outer membrane proteins with amide groups, urease and peptidoglycan for adapt to microenvironment, persistent infection, bacterium–host interac-

tion and pathogenesis [46,47]. Thus, to identify these molecules of *H. pylori* observed as SERS signals by this method and to investigate the kinetics of these molecules are necessary for understanding the development of *H. pylori*-associated disorders. So far, the components of *H. pylori* mentioned above are thought to be candidate molecules by SERS as follows; peptidoglycan, main component of cell wall, UreA and UreB proteins, Apo protein of urease, and outer membrane proteins including BabA and SabA, bacterial adhesion

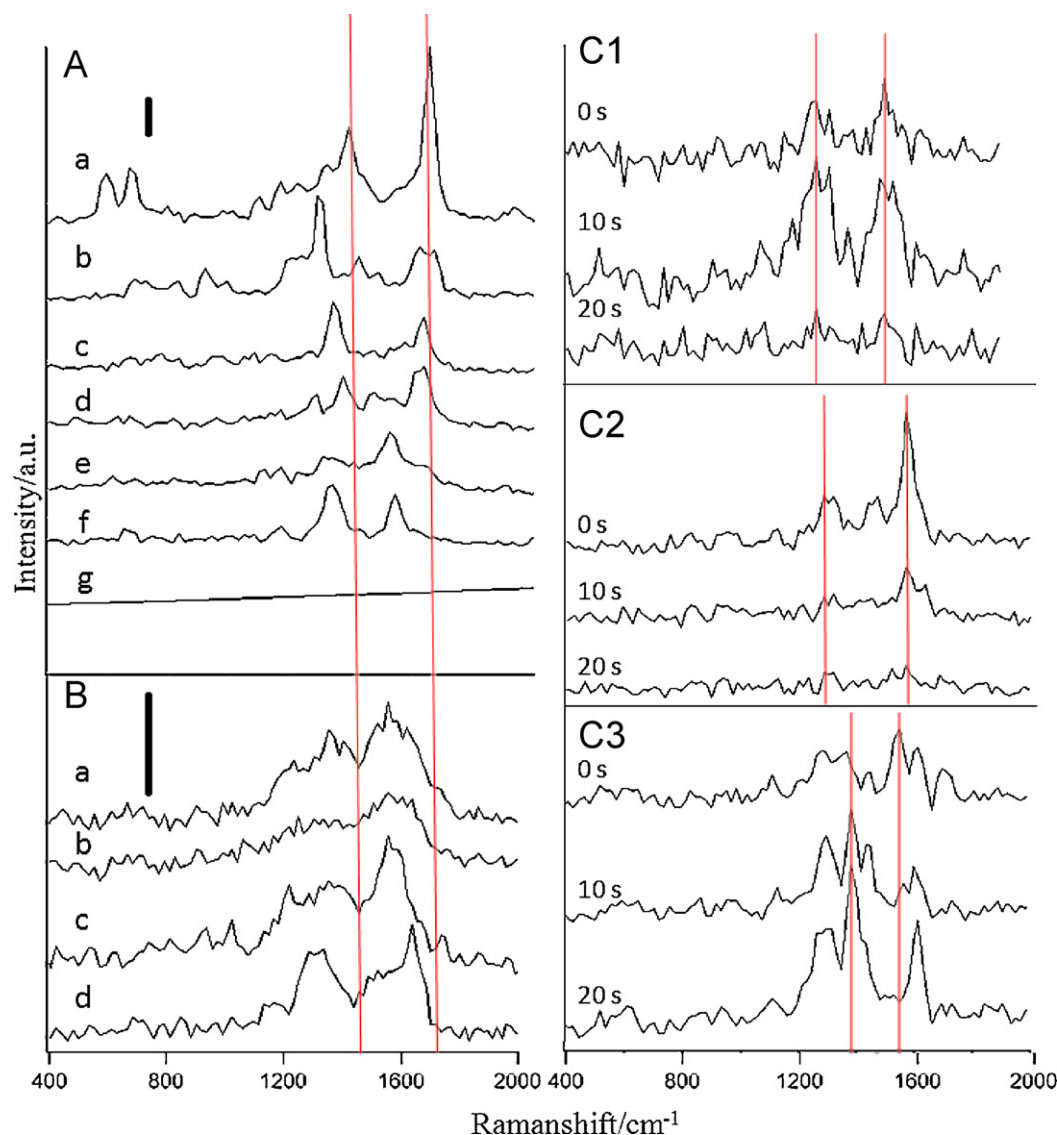


Fig. 2. (A) “a”–“f” SERS spectra from different bright spots and “g” SERS spectra from non bright spot on a bacterial aggregate as indicated in Fig. 1(f). (B) “a”–“d” SERS spectra from different bright spots on a bacterial aggregate without citric acid. Scales of (A) and (B) are 100 counts. (C1–C3) Temporal changes in SERS spectra from three SERS spots as indicated in Fig. 1(f).

proteins of *H. pylori* [48,49]. For next future study, we are analyzing with the isogenic mutants [32,33] derived from *H. pylori* HPK5 strain to elucidate these candidate molecules, which will provide new insights for infectious diseases and evaluate the attribution of SERS to medical field. In this study, many SERS spectra mainly show only two bands around 1300 and 1600 cm^{-1} those are tentatively attributed to amide groups. However, previous reports of SERS from bacterium such as *Escherichia coli* show various Raman bands around 400–1700 cm^{-1} those are attributed to CH_2 rocking, phenylalanine skeletal and so on [45,50]. We consider that the reason for the difference in variations in SERS bands between previous reports and the present our results may be due to the style of adsorption of Ag NPs on cell surfaces. In previous reports, they mixed Ag colloidal solution and cell dispersion liquid and incubated until the adsorption of Ag NPs on cell surfaces. Thus, Ag NPs may be attached on cell surfaces with physical adsorption. On the other hand, we directly synthesized Ag NPs by photo-reduction on cell surfaces. Thus, Ag^+ s are reduced by citric acid at cell surfaces with high affinity points with Ag atoms such as amide groups. The reduced Ag^+ s grow up into Ag clusters and finally form Ag NPs at cell surfaces. The chemical reactivity of

Ag atom clusters is larger than bulk Ag [51]. Thus, we consider that Ag NPs form chemical bonding with cell surfaces compounds through amide groups. In physical adsorption, SERS spectra show all Raman bands by EM enhancement as shown in the previous report [8], however SERS spectra of molecules that are attached on Ag NPs with chemical bonding show relatively strong bands of chemical bands around nitrogen atoms in amide groups by chemical enhancement [16,17]. As indicated in Section 1 the origin of chemical enhancement is a decrease of energy gap between S_0 and S_1 by mixing electronic orbital of molecules and Ag surfaces [15]. Chemical enhancement is sensitive to molecular orientations on Ag NPA surfaces because the orientations vary the amount of decrease in the energy gap [13]. Thus, we consider that observed spectral fluctuation of two SERS bands of amide groups around 1252–1388 cm^{-1} and 1522–1654 cm^{-1} is due to changing in mixing of electronic orbital of metal and that of molecules and the changing is induced by variations in molecular orientations. To test the effect of chemical bonding between Ag NPA surfaces and cell surface molecules, we synthesized Ag NPs by photo-reduction on cell surfaces using 5 mM of Ag nitrate solution without citric acid. We expected two results 1: larger inhomogeneity in chemical bonding

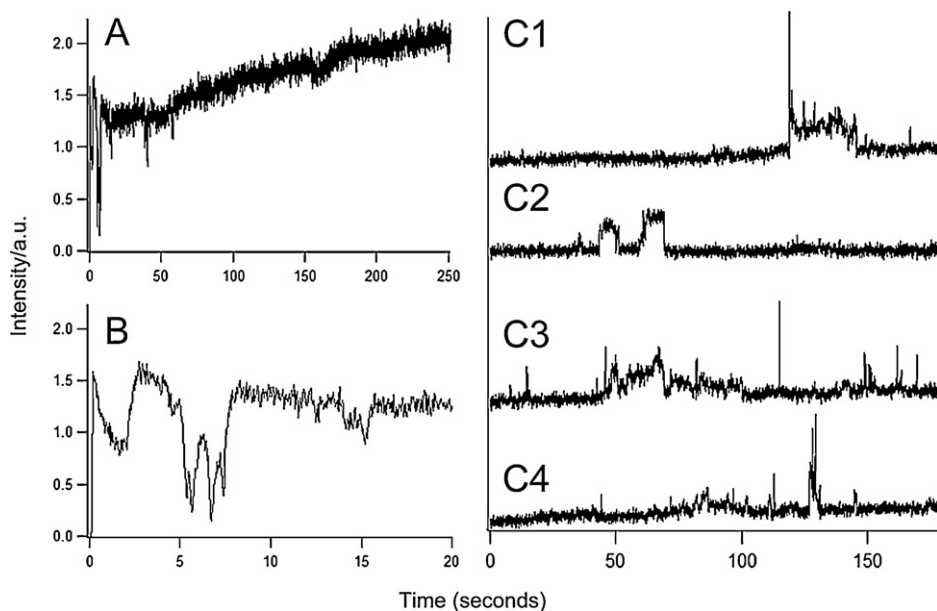


Fig. 3. (A) Temporal changes change in the total SERS light intensity from the beginning of laser irradiation on a bacterial aggregate. (B) Temporal changes change in the total SERS light intensity from the beginning of laser irradiation picked from (A). (C1–C4) Blinking of SERS light intensity of four individual SERS light spots as indicated in Fig. 1(f).

because various cell surface molecules should directly reduce Ag^+ s and form chemical bonding with Ag NPs and 2: disappearance of weak SERS bands in Fig. 2A “a”–“f” because chemical enhancement, which requires chemical bonding between molecules and Ag surfaces, becomes more dominant. SERS spectra of Ag NPs synthesized without citric acid are indicated Fig. 2B “a”–“d”. We observed only two bands those are much broader than those in Fig. 2A “a”–“f”. The broader SERS bands and disappearance of weak SERS bands are consistent to our expectations and thus may indicate that increase in chemical enhancement by inhomogeneous chemical bonding between Ag NPs and cell surface molecules due to the absence of citric acid.

Time-resolved SERS spectra were also measured from the photo-reduced Ag NPs on the HPA. We continuously illuminated green laser during the measurements. Fig. 2C1–C3 shows the temporal changes in SERS spectra from three different SERS-active spots within the time period of 20 s. Interestingly, all SERS spectra show large temporal changes, for example Fig. 2C1 shows that the bands at 1388 and 1654 cm^{-1} increase and decrease, Fig. 2C3 shows that the bands at 1388 and 1654 cm^{-1} shift to higher wavenumber regions. The temporal changes in SERS bands are similar to spot-by-spot variations in SERS spectra as shown in Fig. 2A. Thus, we consider that temporal changing in SERS spectra was also induced by fluctuations in molecular orientations on Ag NPA by molecular thermal diffusion which changes chemical enhancement. Note that the observation of the spectral and temporal variations may be the evidence of detections of single or a few molecules in the present measurements.

To quantitatively evaluate SERS enhancement factors, SERS intensity (photocount) was converted into cross-section (cm^2) using reference data of a gold nanosphere (80 nm in diameter), whose scattering intensity and scattering cross-section is known. We assumed that present SERS signals are from single molecules, because observed spectral fluctuation in Fig. 2 and blinking (will be discussed in Fig. 3) are possible evidence of near single molecule detections. The conversion factor is 1.77×10^{-20} ($\text{cm}^2/\text{photocount}$) under our experimental condition. Thus, the estimated SERS cross-section of amide bands is $1.77 \times 10^{-18}\text{ cm}^2$. A reported differential Raman cross-section of amide bands is $60\text{ mbarn molecule}^{-1}\text{ sr}^{-1}$ at 206.5 nm excitation-wavelength [52].

The differential Raman cross-section was changed into Raman cross-section of $4.46 \times 10^{-29}\text{ cm}^2$ under our experimental condition (532 nm in excitation-wavelength, 0.7 in NA of detection objective lens). Thus, SERS enhancement factors are $\sim 10^{11}$. Note that EM enhancement factors of Raman cross-section is up to $\sim 10^8$ by plasma resonance of Ag NPA [12]. Thus, we consider that additional SERS enhancement factors $< \sim 10^3$ may be due to chemical one, which selectively works on amide groups. The value of chemical enhancement factors are within reported ones [15]. Furthermore, we consider that absence of SERS bands of other functional groups are due to the selective chemical enhancement by a factor of $\sim 10^3$ only for amide groups.

Finally, we measured the time dependence of total SERS intensity from HPA to determine the suitable measurement time. Fig. 3A shows that the total amount of SERS light from one HPA as indicated in Fig. 1d gradually increased with time. The gradual increasing in total SERS intensity means increasing in number of SERS active spots because laser irradiation induces photo-reduction of Ag nitrate and continues to produce Ag NPs which have SERS active nanogaps. Fig. 3B shows the time dependence extracted from Fig. 3A within 20 s to check the initial temporal behavior of the total SERS intensity. At the beginning of SERS light generation, total SERS light was quite instable. Indeed, most of detected light from HPAs within 10 s is not SERS light but autofluorescence of cells. The autofluorescence is rapidly quenched within several second by laser irradiation. Ag NPs were gradually synthesized onto the surface of HPA after 10 s of laser irradiation. In short, we should wait for 10 s before SERS measurements to avoid autofluorescence of cells and to settle stable conditions for SERS measurements. Next we measured the temporal changes in SERS intensity of individual SERS active spots. Fig. 3C shows the temporal changes of SERS intensity of four individual SERS active spots. In all SERS active spots, SERS light randomly changed in the intensity and show blinking. For example, Fig. 3C1 shows rapid increase (at 120 s) and slow fluctuation (for 120–150 s) in SERS intensity. Fig. 3C2 shows square wave like SERS intensity profiles for 40–50 s and for 60–70 s. Fig. 3C3 and C4 shows slow fluctuation with blinking in SERS intensity. Note that we never observed gradual increase in SERS light intensity such as total SERS intensity in Fig. 3A. All temporal changes in SERS intensity of single spots show blinking. The blinking behavior sug-

gests that the SERS light from each spot is from single or a few molecules.

In this study, we proposed a simplified and convenient SERS spectroscopic method of bacteria (*H. pylori*) having low affinity with Ag surfaces. The method is composed of synthesis of Ag NPAs by photo-reduction on HPA surfaces and SERS detections using one green laser beam. We got detectable intensity of SERS spectra of surface molecules of HPAs after 10 s of the photo-reduction. The SERS bands are tentatively attributed to amide groups in surface molecules of HPAs. The selective detections of amide groups indicated that a chemical enhancement mechanism plays an important role in the SERS detections. All SERS spots show large spectral and temporal fluctuations. The fluctuations indicated that the SERS signals may be from near single molecules. The SERS enhancement factors in current study are estimated to be $\sim 10^{11}$. EM enhancement factors may be up to 10^8 by plasma resonance of Ag NPA. Thus, the chemical enhancement factors is may be $< \sim 10^3$ in the present SERS active system. For the next study, we will carry out the SERS spectral analysis of the isogenic mutants [32,33] derived from *H. pylori* HPK5 strain to identify the molecules detected by the present SERS measurements. The identification will provide new insights for infectious diseases and evaluate the attribution of SERS to medical field.

Acknowledgements

This work was supported by Scientific Research (19049013) on Priority Area "Strong Photons-Molecules Coupling Fields (470)", Grant-in-Aid for Scientific Research B (20510111), and C (21310071) from The Ministry of Education, Culture, Sports and Science and Technology (MEXT) of Japan.

References

- [1] T.G. Spiro, Biological Applications of Raman Spectroscopy, John Wiley & Sons Ltd., New York, 1988.
- [2] Y.-S. Huang, T. Karashima, M. Yamamoto, H. Hamaguchi, Biochemistry 44 (2005) 10009.
- [3] K. Kneipp, Y. Wang, H. Kneipp, L. Perelman, I. Itzkan, R.R. Dasari, M. Feld, Phys. Rev. Lett. 78 (1997) 1667.
- [4] S. Nie, S. Emory, Science 275 (1997) 1102.
- [5] H. Xu, E. Bjerneld, M. Käll, L. Borjesson, Phys. Rev. Lett. 83 (1999) 4357.
- [6] K. Imura, H. Okamoto, M. Hossain, M. Kitajima, Nano Lett. 6 (2006) 2173.
- [7] M. Inoue, K. Ohtaka, J. Phys. Soc. Jpn. 52 (1983) 3853.
- [8] M. Moskovits, Rev. Mod. Phys. 57 (1985) 783.
- [9] H. Xu, X. Wang, M.P. Persson, H.Q. Xu, M. Käll, P. Johansson, Phys. Rev. Lett. 93 (2004) 243002.
- [10] T. Itoh, K. Yoshida, V. Biju, Y. Kikkawa, M. Ishikawa, Y. Ozaki, Phys. Rev. B 76 (2007) 085405.
- [11] K. Yoshida, T. Itoh, V. Biju, M. Ishikawa, Y. Ozaki, Phys. Rev. B 79 (2009) 085419.
- [12] K. Yoshida, T. Itoh, H. Tamaru, V. Biju, M. Ishikawa, Y. Ozaki, Phys. Rev. B 81 (2010) 115406.
- [13] J.R. Lombardi, R.L. Birke, T. Lu, J. Xu, J. Chem. Phys. 84 (1986) 4174.
- [14] A. Otto, I. Mrozek, H. Grabhorn, W. Akemann, J. Phys.: Condens. Matter 4 (1992) 1143.
- [15] A. Campion, P. Kambhampati, Chem. Soc. Rev. 27 (1998) 241.
- [16] T. Itoh, K. Hashimoto, V. Biju, M. Ishikawa, B.R. Wood, Y. Ozaki, J. Phys. Chem. B 110 (2006) 9579.
- [17] D. Wu, J. Li, B. Ren, Z. Tian, Chem. Soc. Rev. 37 (2008) 1025.
- [18] A. Sujith, T. Itoh, H. Abe, A.A. Anas, K. Yoshida, V. Biju, M. Ishikawa, Appl. Phys. Lett. 92 (2008) 103901.
- [19] A. Sujith, T. Itoh, H. Abe, K. Yoshida, M.S. Kiran, V. Biju, M. Ishikawa, Anal. Bioanal. Chem. 394 (2009) 1803.
- [20] J. Kneipp, H. Kneipp, M. McLaughlin, D. Brown, K. Kneipp, Nano Lett. 6 (2006) 2225.
- [21] L. Zeiri, B.V. Bronk, Y. Shabtai, J. Eichler, S. Efrima, Appl. Spectrosc. 58 (2004) 33.
- [22] J.A. Dieringer, R.B. Lettan II, K.A. Scheidt, R.P. Van Duyne, J. Am. Chem. Soc. 129 (2007) 16249.
- [23] Y.C. Cao, R. Jin, C.A. Mirkin, Science 297 (2002) 1536.
- [24] X. Qian, X.H. Peng, D.O. Ansari, Q.Y. Goen, G.Z. Chen, D.M. Shin, L. Yang, A.N. Young, M.D. Wang, S.M. Nie, Nat. Biotechnol. 26 (2007) 83.
- [25] J.N. Anker, W.P. Hall, O. Lyandres, N.C. Shah, J. Zhao, R.P. Van Duyne, Nat. Mater. 7 (2008) 442.
- [26] J.F. Li, Y.F. Huang, Y. Ding, Z.L. Yang, S.B. Li, X.S. Zhou, F.R. Fan, W. Zhang, Z.Y. Zhou, D.Y. Wu, B. Ren, Z.L. Wang, Z.Q. Tian, Nature 464 (2010) 392.
- [27] M.S. Kiran, T. Itoh, K. Yoshida, N. Kawashima, V. Biju, M. Ishikawa, Anal. Chem. 82 (2010) 1342.
- [28] R. Aroca, Surface-Enhanced Vibrational Spectroscopy, John Wiley & Sons Ltd., Chichester, 2006.
- [29] K. Kneipp, M. Moskovits, H. Kneipp, Surface-Enhanced Raman Scattering – Physics and Applications, Springer, Heidelberg/Berlin, 2006.
- [30] N. Uemura, S. Okamoto, S. Yamamoto, N. Matsumura, S. Yamaguchi, M. Yamakido, K. Taniyama, N. Sakaki, R.J. Schlemper, N. Engl. J. Med. 345 (2001) 784.
- [31] H. Takeuchi, M. Shirai, J.K. Akada, M. Tsuda, T. Nakazawa, J. Bacteriol. 180 (1998) 5263.
- [32] H. Takeuchi, T. Nakazawa, T. Okamoto, M. Shirai, M. Kimoto, M. Nishioka, S.A. Con, N. Morimoto, T. Sugiura, Microbiol. Immunol. 50 (2006) 487.
- [33] V.T. Trang, H. Takeuchi, H. Kudo, A. Aoki, S. Katsuno, T. Shimamura, T. Sugiura, H. Ukeda, J. Agric. Food Chem. 57 (2009) 11343.
- [34] P.C. Lee, D. Meisel, J. Phys. Chem. 86 (1982) 3391.
- [35] T. Itoh, Y. Kikkawa, K. Yoshida, K. Hashimoto, V. Biju, M. Ishikawa, Y. Ozaki, J. Photochem. Photobiol. A: Chem. 183 (2006) 322.
- [36] E.J. Bjerneld, K.V.G.K. Murty, J. Prikulis, M. Käll, ChemPhysChem 3 (2002) 116.
- [37] T. Hatling, Y. Alaverdyan, M.T. Wenzell, R. Kullock, M. Käll, L.M. Eng, J. Phys. Chem. C 112 (2008) 4920.
- [38] T. Itoh, V. Biju, M. Ishikawa, S. Ito, H. Miyasaka, Appl. Phys. Lett. 94 (2009) 144105.
- [39] M. Kerker, O. Siiman, L.A. Bumm, D.-S. Wang, Appl. Opt. 19 (1980) 3253.
- [40] X. Wang, T. He, H. Wen, C. Xu, J. Zuo, F. Liu, Spectrochim. Acta Part A 53 (1997) 1411.
- [41] X.J. Yuan, H.M. Gu, J.W. Wu, J. Mol. Struct. 977 (2010) 56.
- [42] J.M. Reyes-Goddard, H. Barr, N. Stone, Photodiagn. Photodyn. Ther. 2 (2005) 223.
- [43] V. Reipa, A. Gaigalas, S. Abramowitz, J. Electroanal. Chem. 348 (1993) 413.
- [44] H. Schulz, M. Baranska, Vib. Spectrosc. 43 (2007) 13.
- [45] K. Maria, P.I. Natalia, N. Reinhard, H. Christoph, Anal. Sci. 26 (2010) 761.
- [46] I.G. Boneca, Curr. Opin. Microbiol. 8 (2005) 46.
- [47] P. Doig, T. Trust, Infect. Immun. 62 (1994) 4526.
- [48] N. Sabarth, R. Hurvitz, M. Schmidt, U. Zimny-Arnd, P.R. Jungblut, T.F. Meyer, D. Bumann, J. Microbiol. Methods 62 (2005) 345.
- [49] S. Odenbreit, Int. J. Med. Microbiol. 295 (2005) 317.
- [50] W.R. Premasiri, D.T. Moir, M.S. Klempner, N. Krieger, G. Jones, L.D. Ziegler, J. Phys. Chem. B 109 (2005) 312.
- [51] H. Nakatsuji, Prog. Surf. Sci. 54 (1997) 1.
- [52] Z. Chi, X.G. Chen, J.S.W. Holtz, S.A. Asher, Biochemistry 37 (1998) 2854.